Samarium magnetism studied on $SmPd_2Al_3$ single crystal

J. Pospíšil,* M. Kratochvílová, J. Prokleška, M. Diviš, and V. Sechovský
Faculty of Mathematics and Physics, Department of Condensed Matter Physics, Charles University, Ke Karlovu 5, 121 16 Prague 2, The Czech Republic

(Received 24 June 2009; revised manuscript received 18 December 2009; published 21 January 2010)

In this paper, specific features of Sm magnetism in an intermetallic compound have been studied. For this purpose, a high-quality single crystal of $SmPd_2Al_3$ was grown and subjected to detailed measurements of specific heat, magnetization, ac susceptibility, and electrical resistivity with respect to temperature and a magnetic field applied along the principal crystallographic directions. $SmPd_2Al_3$ magnetism was found to be strongly anisotropic with the easy-magnetization direction along the c axis where the main magnetic features are concentrated. The a-axis response remains weak, paramagneticlike, even in the magnetically ordered state. Ferromagnetism with $T_C=12.4$ K has been indicated by all the measured physical properties. At lower temperatures, three successive order-order phase transitions have been observed on the temperature dependence of the specific heat as three anomalies: at 3.4, 3.9, and 4.4 K, respectively. The low-temperature magnetization data can be understood within a scenario that considers the antiferromagnetic ground state as being gradually destroyed through a series of four metamagnetic transitions at 0.03, 0.35, 0.5, and 0.75 T, as detected in the 1.8 K magnetization data. The temperature dependence of the paramagnetic susceptibility below 200 K can be in the first approximation interpreted in terms of a Curie-Weiss law modified by temperature-independent Van Vleck contribution due to the low-lying first excited multiplet $J=7/2$ being populated. At higher temperatures, involvement of the second excited multiplet $J=9/2$ should also be considered. The experimental data are discussed together with the results of electronic-structure and crystal-field calculations from first principles, which were performed as an important part of the study for comprehension and explanation of the observed behavior of the $SmPd_2Al_3$ compound.

DOI: 10.1103/PhysRevB.81.024413 PACS number(s): 75.30.−m, 75.40.Cx

I. INTRODUCTION

The localized $4f$-electron magnetism of lanthanide ions is by rule characterized by stable magnetic moments, which reflect the population of energy levels of the ground-state multiplet determined by total angular momentum J and split by crystal-field (CF) interaction. Paramagnetic susceptibility (χ) well above the magnetic-ordering temperature obeys the Curie-Weiss law. This behavior may be modified at lower temperatures in the case of a considerable CF interaction. Sm represents an exception to this rule: Sm magnetism is not governed only by the ground-state multiplet $J=5/2$ since the first (and second) excited multiplet $J=7/2$ ($J=9/2$) has only an energy of 0.1293 eV (0.2779 eV).[1] Therefore the temperature dependence of paramagnetic susceptibility at temperatures up to about 400 K is influenced by populating the CF split levels of the first and second excited multiplets via the temperature-independent Van Vleck terms[2] and does not obey the Curie-Weiss law. A typical $1/\chi$ vs T plot for a Sm compound is strongly nonlinear and usually exhibits a maximum around 400 K, which is very sensitive to CF and exchange interaction.[3] Since the samarium magnetic moment at low temperatures is small ($gJ=0.71\mu_B$ for the Sm^{3+} free ion) exchange interactions can be very peculiar and several magnetic phases may appear in the same material at different temperature and magnetic-field intervals, respectively. In the present paper we demonstrate some specific features of Sm magnetism from the results of our recent study of a high-quality single crystal of the compound $SmPd_2Al_3$. We focused our attention on measurements of magnetization (M), ac susceptibility (χ_{ac}), specific heat (C_p), and electrical resistivity (ρ) as functions of temperature (T) and the external magnetic field (B). The anisotropy of magnetic properties has been determined from measurements in magnetic fields applied along the principal crystallographic directions [100] and [001]. Along with our experimental work, we performed various theoretical calculations of the electronic structure and CF parameters and compared calculated results with experimental findings. $SmPd_2Al_3$, as well as its $REPd_2Al_3$ (RE=La,Ce,Nd,Gd) counterparts, adopt the same hexagonal $PrNi_2Al_3$-type crystal structure.[4] It is worth noting that the U isostructural analog, UPd_2Al_3, is a well-known heavy-fermion antiferromagnetic superconductor ($\gamma=150$ mJ K^{-2} $mole^{-1}$, $T_C=2$ K, and $T_N=14$ K).[5] The nonmagnetic analog $LaPd_2Al_3$ becomes superconducting at 0.8 K.[6] The susceptibility of the Ce, Pr, and Nd compounds obeys the Curie-Weiss law at temperatures above 100 K.

Deviations from the Curie-Weiss law at temperatures below T_C are apparently due to CF splitting of the ground-state multiplet,[7] which is also reflected in the Schottky anomaly observed in specific-heat data collected for $CePd_2Al_3$ and $PrPd_2Al_3$.[8] $CePd_2Al_3$ exhibits heavy-fermion behavior at low temperatures ($\gamma=380$ mJ K^{-2} $mole^{-1}$) with a Kondo effect;[9] nevertheless, it becomes antiferromagnetic below 2.8 K.[10,11] $PrPd_2Al_3$ remains paramagnetic down to 1.5 K. Saturation of susceptibility below 15 K has been attributed to the CF effect yielding the ground-state singlet.[12] $NdPd_2Al_3$ becomes antiferromagnetic at $T_N=6.5$ K as reported in Ref. 8. The value of T_N of $NdPd_2Al_3$ has been found to be varying in the interval from 5.2 to 7.7 K for various samples, following a linear dependence on the lattice parameter a, not on c, which may be understood with the exchange interactions inside the ab plane dominating the magnetism in this compound.[11] The

most intriguing case in the $RE\mathrm{Pd}_2\mathrm{Al}_3$ family seems to be $\mathrm{SmPd}_2\mathrm{Al}_3$. Results published so far on $\mathrm{SmPd}_2\mathrm{Al}_3$ have been obtained by measuring only polycrystals and point to a complex magnetic phase diagram with several magnetic phase transitions below 12 K.[4] The CF interaction in $\mathrm{SmPd}_2\mathrm{Al}_3$ can be reasonably estimated by considering the well-determined CF parameters for the $\mathrm{NdPd}_2\mathrm{Al}_3$ compound[13,14] or by using CF calculations as obtained from first principles, as will be presented in this paper. Specific-heat measurements of $\mathrm{SmPd}_2\mathrm{Al}_3$ have been reported revealing anomalies at 3, 6, and 12 K, indicating magnetic phase transitions.[8] From susceptibility data three magnetic phase transitions at 4, 4.3, and 12 K,[4] respectively, have been proposed whereas the electrical resistivity reflects strongly a magnetic phase transition at 12 K,[4] typical for a transition to ferromagnetic ordering, the peaklike anomaly around 3.5 K resembles a transition to a low-temperature antiferromagnetic phase.[10] The magnetization curve measured at 2.5 K indicated two magnetic phase transitions (at approximately 0.3 and 2 T).[10] It is clear that $\mathrm{SmPd}_2\mathrm{Al}_3$ presents unique case of $4f$ magnetism and we attempt here to put this context together with previous results and Sm magnetism generally.

II. EXPERIMENTAL AND COMPUTATIONAL DETAILS

The single crystal of $\mathrm{SmPd}_2\mathrm{Al}_3$ was grown in a triarc furnace by the Czochralski pulling method from stoichiometric amounts of elements. The single crystal was a 20-mm-long cylinder with a diameter of 3–4 mm. Crystal quality was checked by the Laue technique. A small part of the crystal was pulverized in an agate grinding mortar and x-ray powder diffraction (XRPD) data were recorded on a Seifert powder diffractometer equipped with a monochromator to provide the Cu $K\alpha$ radiation. The XRPD data were analyzed by means of the Rietveld profile procedure[15] using the program FULLPROF.[16] The final composition of the crystal was checked by EDX (energy-dispersive x-ray analysis) on a FE-scanning electron microscopy Tescan. The Laue technique was also used for crystal orientation. Samples appropriate by shape for the magnetization and specific-heat measurements were cut by a fine wire saw (South Bay Technology Inc., type 810). The sample for the magnetization measurements had the form of a small beam ($1\times1\times1.5$ mm^3) with the rectangular planes oriented perpendicular to the crystallographic axes a and c, respectively. The specific-heat samples were small plates ($1.5\times1.5\times0.2$ mm^3) with the main-plate plane perpendicular to the a and c axes, respectively. The orientation of each prepared sample was subsequently revised again by Laue technique. The specific-heat, ac susceptibility, and magnetization measurements were performed using the Quantum Design Physical Property Measurement System and the Magnetic Property Measurement System, respectively. The specific heat was measured at temperatures from 1.8 to 300 K in magnetic fields up to 9 T. The magnetization was measured in a temperature range from 1.8 to 400 K and in magnetic fields 0–14 T. The ac susceptibility was measured from 1.8 to 30 K in an ac magnetic field 0.03 mT with a frequency of 497 Hz. The magnetic field was applied along the a and c axes, respectively. To obtain direct information about the ground-state electronic structure and magnetic properties, we applied theoretical methods from first principles. The ground-state electronic structure was calculated on the basis of density-functional theory (DFT) within the local spin-density approximation (LSDA) (Ref. 17), and generalized gradient approximation (GGA).[18] For this purpose, we used the full-potential augmented plane wave plus local-orbitals method (APW+lo) as implemented in the latest version (WIEN2K) of the original WIEN code.[19] The calculations were scalar relativistic and performed with the following parameters: nonoverlapping atomic spheres (AS) radii of 2.8, 2.5, and 2.0 a.u. (1 a.u.=52.91 pm) were taken for Sm, Pd, and Al, respectively; the basis for the expansion of the valence electron states less than 6 Ry below the Fermi energy) consisted of more than 800 basis functions (more than 130 APW/atom) plus Sm ($5s$,$5p$), Pd ($4p$), and Al ($2p$) local orbitals. The results of our experimental analysis suggest that the $4f$ electrons are localized atomiclike. Therefore the Sm $4f$ states were treated in an open-core approximation with the stable atomic configuration $4f^5$. The wave functions in the AS region were expanded up to $l=12$ and a density GMAX=14 was used for the interstitial charge. Brillouin-zone (BZ) integration was performed with the tetrahedron method[19] on a 270 special k-point mesh (4600 k points in the full BZ). We carefully tested the convergence of the results presented with respect to the parameters mentioned and found them to be fully sufficient for all the presented characteristics of the $\mathrm{SmPd}_2\mathrm{Al}_3$ compound. We also analyzed the temperature evolution of the magnetic entropy. In addition we included spin-orbit coupling into the calculations for the electronic structure of the valence states (delocalized Bloch states); we found only minor changes in the density of states (DOS) curves and calculated crystal-field parameters. The calculations of first principles of the crystal-field interaction were performed using the method described in Ref. 20. In these calculations the electronic structure and corresponding distribution of the ground-state charge density was obtained using the full-potential APW+lo method. The CF parameters originated from the aspherical part of the total single-particle DFT potential in the crystal. To eliminate self-interaction, a self-consistent procedure was first converged with the $4f$ electrons in the core,[20] which was the open-core approximation used in this work. To diagonalize the microscopic CF Hamiltonian of the hexagonal point group symmetry, we used $J=5/2$, $J=7/2$, and $J=9/2$ multiplets and Wybourne parameterization of the CF matrix elements.[21] Therefore the J mixing and the intermediate-coupling many-particle $4f$-wave functions were properly taken into account. The CF perturbation matrix had a dimension of 24 and the resulting eigenenergies and eigenfunctions were used to calculate the magnetic susceptibility as a function of temperature.

III. RESULTS

We successfully prepared the $\mathrm{SmPd}_2\mathrm{Al}_3$ single crystal of high quality as confirmed by the Laue patterns. The XRPD data contained only the reflections compatible with a hexagonal structure of the $\mathrm{PrNi}_2\mathrm{Al}_3$ type (space group $P6/mmm$) with lattice parameters $a=5.293$ Å, $c=4.064$ Å,

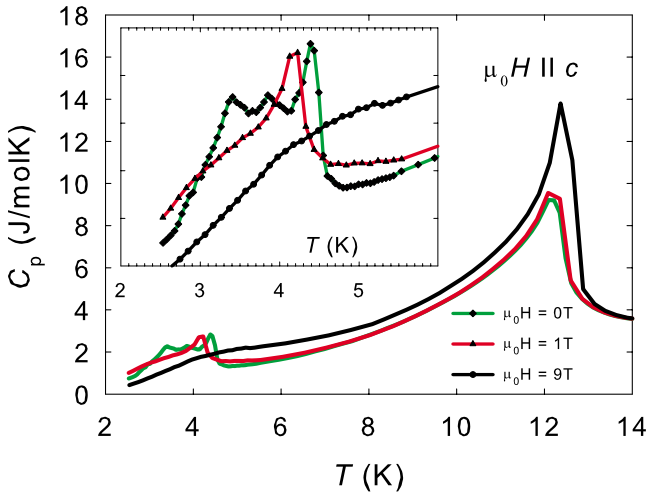

FIG. 1. (Color online) Temperature dependence of specific heat measured in various magnetic fields applied parallel to the c axis. The inset shows details of the low-temperature anomalies.

which are in good agreement with published data. The proper 1:2:3 stoichiometry of the grown crystal was confirmed by EDX analysis within the accuracy of the method. No spurious phase has been located. We also carried out an area analysis and concentrations gradients were also studied. No concentration gradients have been detected.

A. Specific heat

The C_P vs T data were collected by two series of measurements in a magnetic field applied along the a and c axes, respectively. In zero magnetic field a large and sharp l-shape anomaly in the $C_P(T)$ dependence, peaking at 12.4 K was detected and three much smaller peaklike anomalies located at 4.4, 3.9, and 3.4 K, respectively (see Fig. 1). We tentatively denote these temperatures as T_C, T_1, T_2, and T_3, respectively. The 12.4 K anomaly became gradually enhanced with increasing magnetic field applied along the c axis ($B \| c$), though it remained "pinned" at nearly the same temperature (it move only very slightly to higher temperatures). Although such evolution is rather unusual, the magnetization and resistivity data presented below confirm that this specific-heat anomaly is apparently associated with the onset of a ferromagnetic ordering in $SmPd_2Al_3$ and 12.4 K is the Curie temperature (T_C) of this material. The low-temperature anomalies, which were smeared out in fields $B \| c$ higher than 1 T, were presumably associated with an order-order magnetic phase transition. The 12.4 K peak remained nearly intact in a magnetic field up to 9 T applied along the a axis (not shown in the figure), thus confirming a strong magnetocrystalline anisotropy in the ferromagnetic state. On the other hand, the low-temperature group of anomalies became continuously smeared out with an increasing field $B \| a$ (not shown in the figure). This result indicates that the low-temperature phases ($T < T_1$) have nonzero components (probably antiferromagnetic) in the basal plane of the hexagonal structure. For proper comparison, in the following discussion of our results along with existing literature data on $SmPd_2Al_3$, we have collected together all existing information (including our results) on the temperatures of anomalies of specific heat, magnetization in very low fields, ac susceptibility, and electrical resistivity in Table I. It is immediately apparent that there is an unambiguous response of all measured properties to the onset of magnetic ordering slightly above 12 K whereas the situation is not so straightforward in the features observed between 3 and 5 K. The temperature dependence of the specific heat of $SmPd_2Al_3$, which is presented over a wide temperature range in Fig. 2, was considered to be a sum of the electronic C_{el}, phonon C_{ph}, magnetic C_{mag}, and Shottky C_{Sch} contribution, respectively,

$$C_p = C_{el} + C_{ph} + C_{mag} + C_{Sch}. \quad (1)$$

The most significant is the phonon contribution mainly at higher temperatures and this contribution was evaluated within the aforementioned Debye and Einstein model,[22] the

TABLE I. Summary of temperatures of anomalies in specific heat, ac susceptibility, low-field magnetization, and electrical resistivity observed in our results in comparison with the parameters of magnetic transitions in $SmPd_2Al_3$ reported in the literature.

		Anomaly location (K)			
Property	Source	T_C	T_1	T_2	T_3
C_p	(This work)	12.4	4.4	3.9	3.4
C_p	Ref. 4	12.5	4.3	4	
C_p	Ref. 8	12.5	4.7		3.7
χ_{ac}	(This work)	12.5	4.5		3.7/3.4
M	(This work)	12.3	4.4		3.4
M	Ref. 10	12.5		4	3.3
M	Ref. 4	12.5	4.3	4	
ρ	(This work)	12.4	4.4		3.4
ρ	Ref. 10	12.5	4.5		3.6
ρ	Ref. 4	12.0			

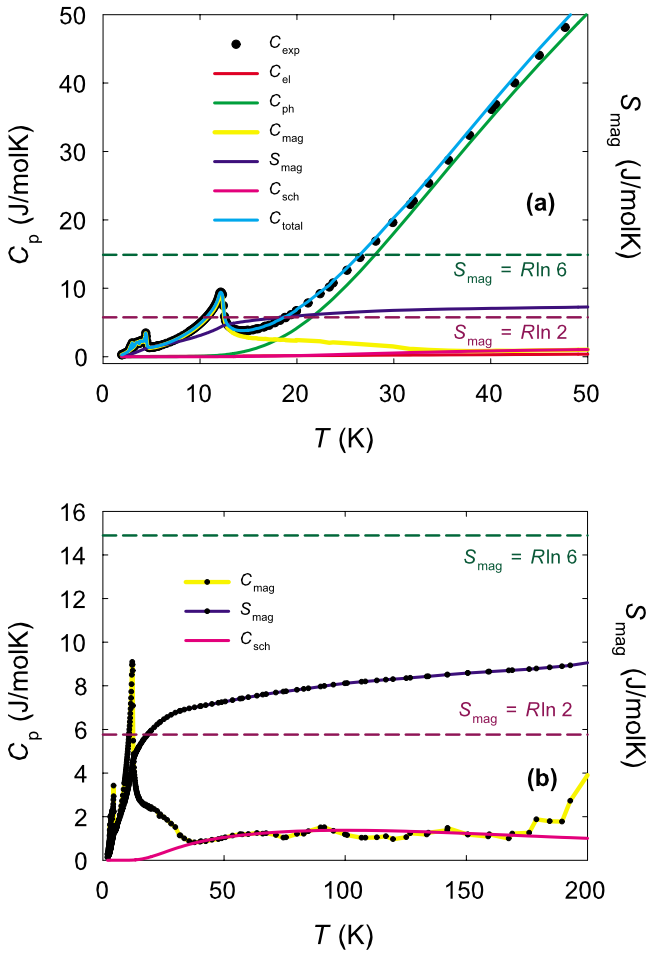

FIG. 2. (Color online) Comparative analysis of specific heat: (a) the graph shows the total specific heat and individual contributions, respectively. (b) Temperature dependence of magnetic entropy is shown, as well.

results being listed in Table II. The values of the phonon contribution have then been subtracted from the raw specific-heat data. As input data for the used model, the values of γ=6.0 mJ/mol K^2,[23] T_D=180 K (Ref. 24) and figures of degeneration of the four phonon optical branches 2-5-3-5,[25] were taken. The remaining values were analyzed by testing all the free parameters in order to reach the best agreement with experimental data based on the equation listed hereafter for the other specific-heat contribution

TABLE II. The values and degeneracy of branches of the phonon contribution to the total specific heat evaluated on the basis of Einstein and Debye models.

Branches	Degeneracy	θ (K)	α (10^{-4} K^{-1})
θ_D		191	5.0
θ_{E1}	2	103	5.0
θ_{E2}	5	210	4.5
θ_{E3}	3	154	4.0
θ_{E4}	5	420	3.0

TABLE III. Energy of the three Kramer's doublets after CF splitting of the degenerated ground state J=5/2 multiplet.

Levels	Energy (K)
Δ_1	0
Δ_2	130 ± 15
Δ_3	300 ± 40

$$C_{ph} = R\left(\frac{1}{1-\alpha_D T}C_D + \sum_{i=1}^{3N-3}\frac{1}{1-\alpha_E T}C_E\right), \tag{2}$$

$$C_{el} = \gamma T, \tag{3}$$

$$C_{Sch} = \frac{R}{T^2}\left\{\frac{\sum_{i=0}^{n}\Delta_i^2 \exp\left(-\frac{\Delta_i}{T}\right)}{\sum_{i=0}^{n}\exp\left(-\frac{\Delta_i}{T}\right)} - \left[\frac{\sum_{i=0}^{n}\Delta_i \exp\left(-\frac{\Delta_i}{T}\right)}{\sum_{i=0}^{n}\exp\left(-\frac{\Delta_i}{T}\right)}\right]^2\right\}. \tag{4}$$

The value found for the Sommerfeld coefficient was γ =7 mJ/mol K^{-2}, which is a typical figure that may be expected and measured in Sm intermetallics compounds.[23] We also analyzed the temperature evolution of the magnetic entropy (Fig. 2). In the temperature range 1.8–20 K we observed a high jump up to the value R ln 2 and we presume that the magnetic ground state of our compound is a doublet. An additional increase in temperature led to a gradual growth of magnetic entropy. The values for entropy should reach the value R ln 6 when the energy of the third doublet is achieved but unfortunately this doublet is above room temperature. We have measured specific-heat data up to 400 K but the data were strongly affected by the transformation of apiezon from temperatures over 250 K and it was inappropriate to solve the absolute value of entropy from the experimental data in this temperature range.

A huge energy gap of 130 K was observed between the ground and the first excited state (see Table III), respectively, which is in good agreement with the findings in Ref. 4 and our theoretical calculations. The existence of a third doublet, indicated to be around room temperature, motivated us to measure magnetization up to 400 K, because a strong influence of CF on the susceptibility behavior was expected, as will be discussed later.

B. ac susceptibility and magnetization

The temperature dependence of the susceptibility measured in the ac magnetic field applied along the a and c axes, respectively, is shown in Fig. 3. The a-axis data were characterized by a very low, nearly temperature-independent signal free of any considerable anomaly exceeding signal noise, whereas the data measured in the ac field applied along the c axis exhibited three anomalies, presumably indicating magnetic phase transitions. When cooling, the c-axis data exhibited a sudden upturn commencing at T_C=12.4 K, a sharp

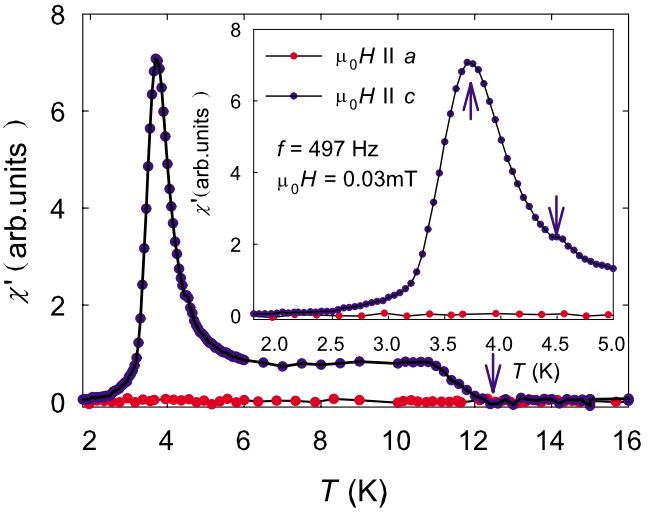

FIG. 3. (Color online) Temperature dependence of ac susceptibility measured with the excitation field applied along the a and c axes. The inset shows detail at low temperature and critical temperatures are emphasized by the arrows.

peak at 3.7 K and a shoulder at 4.5 K. The latter two features may be tentatively associated with the magnetic phase transitions at T_2 and T_1, respectively, which is tentatively implied on comparing the data in Table I.

The theory,[26] however, says that T_N, the temperature at the maximum of the specific heat and the maximum in $\partial(\chi T)/T$ vs T frequently does not coincide with the maximum in χ vs T in real systems. That was also the case in our study where the maximum in $\partial(\chi T)/T$ vs T was at 3.4 K, which coincided with the T_N value determined from specific-heat data. The dramatic difference between the magnetization curves measured at 1.8 K in the magnetic field applied along the a and c axes, respectively (Fig. 4) corroborated, in agreement with the specific-heat and ac susceptibility data, the conclusion that the magnetocrystalline anisotropy in $SmPd_2Al_3$ was uniaxial and the easy-magnetization direction was the crystallographic c axis. Whereas the magnetic moment in the field $B \| c$ is dominant and saturates above 2 T, a very weak

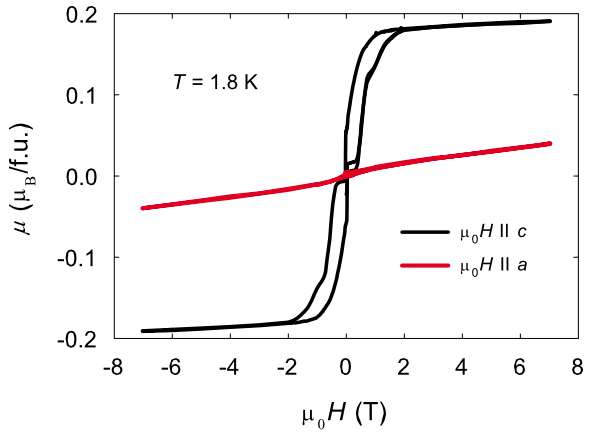

FIG. 4. (Color online) Hysteresis loops measured at temperature 1.8 K with applied magnetic field parallel and perpendicular on the basal plane.

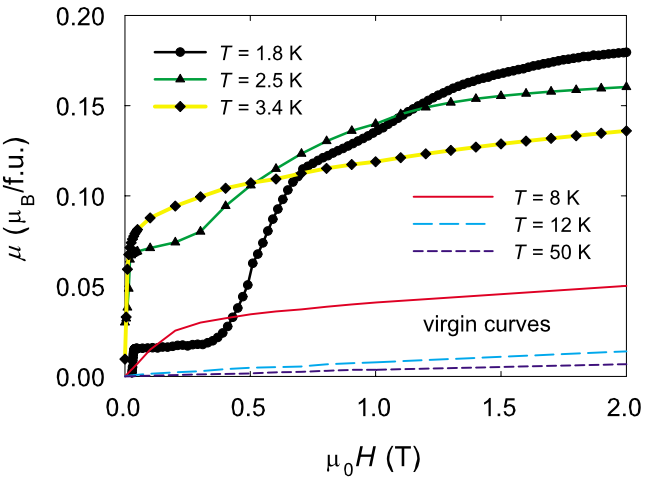

FIG. 5. (Color online) The figure shows virgin curves of $SmPd_2Al_3$ measured along the easy-magnetization axis and their temperature evolution.

paramagneticlike linear (in higher fields) response is observed for $B \| a$. The slight nonlinearity and hysteresis observed in the loop measured along the hard-magnetization axis was considered to be no more than the result of an imperfect geometry in the experiment and slight misorientation of the sample than some intrinsic hard axis behavior. The c-axis magnetic moment of 0.19 μ_B/f.u. at 1.8 K observed in a field of 7 T is nearly five times lower than the expected ordered moment for the ground-state multiplet of the free Sm^{3+} ion ($gJ\mu_B = 0.71\mu_B$), which is presumably responsible for the entire magnetic behavior of $SmPd_2Al_3$. We roughly estimated the observed magnetic moment of the ground state from crystal-field calculations. We obtained a semiquantitative agreement with the experimentally observed magnetization at 1.8 K. For simplicity, we did not include the exchange interaction due to its complex nature. The steplike shape of the c-axis curve in fields weaker than 2 T was fully reproducible and is apparently connected with the specific features of samarium magnetism in $SmPd_2Al_3$. A detailed view of the magnetization loops for $B \| c$ is presented in Fig. 5.

A series of four metamagneticlike transitions can be identified on the 1.8 K virgin magnetization curve. The onsets of transitions denoted by arrows can be found at 0.03, 0.35, 0.5, and 0.75 T, respectively. The transitions in lower fields can still be traced on the curve measured at 2.5 K but they have already gone at temperatures 3.4 K and higher. The magnetization loops measured at 1.8 and 2.5 K exhibited not only some metamagneticlike features but also pronounced hysteresis. All these features vanished at temperatures from 3.4 K. This implies that the ground-state phase, which forms at T_3 is antiferromagnetic and apparently rather complicated. The magnetization curves measured at $T_3 < T < T_C$, however, still showed a strong tendency to saturate as usually found in ferromagnets. The Arrott-plot analysis of the magnetization curves confirmed the value of $T_C = 12.4$ K. Above this temperature, the typical paramagnetic response of the magnetization to the magnetic field applied parallel to the c axis was observed. In fields parallel to the a axis, the magnetization

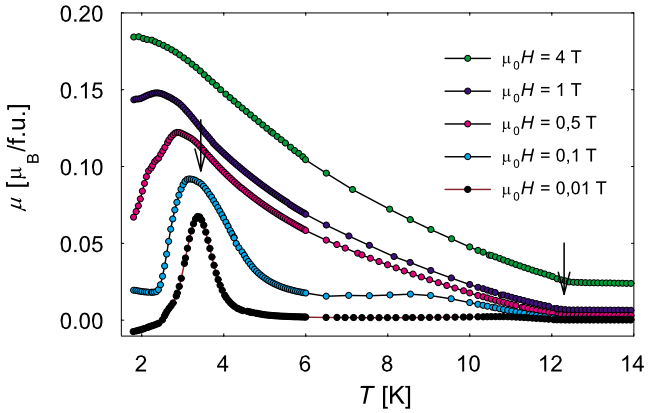

FIG. 6. (Color online) Temperature dependence of magnetic moment of $SmPd_2Al_3$ measured in selected magnetic fields applied along the c with increasing temperature from the low-temperature ZFC state.

remained and very weak and nearly temperature independent below T_C irrespective of the dramatic developments in the c-axis magnetization. We also measured the temperature dependence of the magnetic moment in several constant magnetic fields applied along the c axis, the results of which are shown in Fig. 6. In very low fields the value of the magnetic moment sharply increased below T_C, which was in a good agreement with the anomaly observed in the specific-heat and ac susceptibility data as well as with the evolution of the magnetization loops with temperature. The 10 mT data were in a reasonable agreement with the ac susceptibility behavior. The evolution of 3.4 K anomaly with the increasing magnetic field, as well as the evolution of the magnetization curves with temperature decreasing below 5 K, resembled a transition to a low-temperature antiferromagnetic state, which is stable only in very low magnetic fields. The bifurcation of the thermomagnetic curve in the zero-field-cooled (ZFC) and FC branches appeared at temperatures below 3.6 K (Fig. 7), where a hysteresis of the magnetization curves also appeared. The bifurcation point shifted to lower tem-

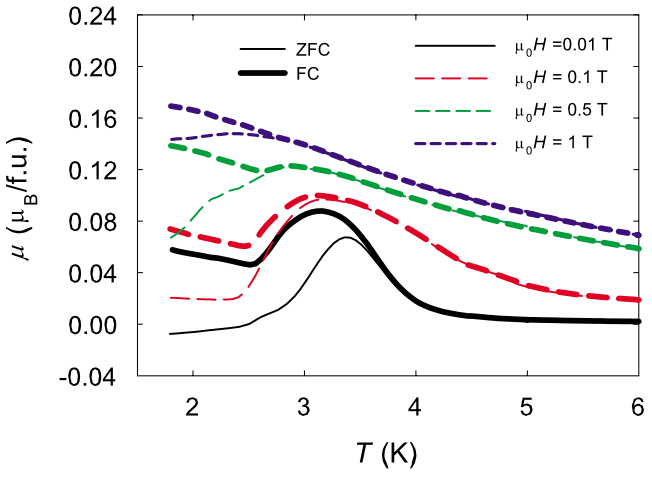

FIG. 7. (Color online) FC and ZFC thermomagnetic curves measured for $SmPd_2Al_3$ measured in selected magnetic fields applied along c.

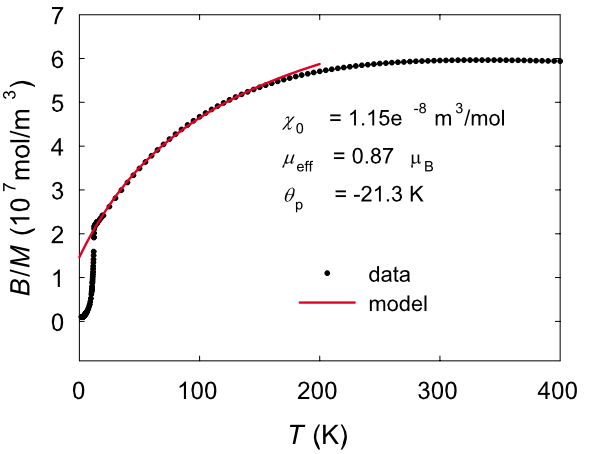

FIG. 8. (Color online) Temperature dependence of inverse susceptibility (B/M) in magnetic field applied along the c axis, respectively. The full line represents the modified Curie-Weiss fit.

peratures with increasing applied magnetic field. However, an alternative interpretation can also be considered. It involves a ferromagnetic component to the magnetic order at the lowest temperature. If all four zero-field ordering transitions are linked to the field-induced transitions, then the lowest-field one may be linked to the ferromagnetic transition at 12.4 K, and would be in fact the coercive field at which the sample becomes a single domain, as far as the ferromagnetic component is concerned. The developing difference (Fig. 7) in zero-field-cooled and field-cooled magnetization can be considered direct evidence of developing coercivity, which in turn is linked to ferromagnetism. The upper three field-induced transitions at 1.8 K may then be directly connected to the zero-field transitions at 3.4, 3.9, and 4.4 K. The internal molecular field can be estimated at 1.8 K as 15 T. This value is roughly comparable with the coercive field. A specific issue of magnetism in $SmPd_2Al_3$ is the involvement of the populated CF levels of the first and the second exited multiplet. This is well documented by the extremely broad Schottky contribution to the specific heat (see Fig. 2), and, in addition, a necessary impact on the magnetization (susceptibility) behavior at elevated temperatures would be expected. The temperature dependence of the inverse susceptibility B/M is strongly nonlinear for both field directions, i.e., it does not follow the Curie-Weiss law. The data in Fig. 8, however, can be well fitted by the modified Curie-Weiss law[27] between 15 and 150 K,

$$\chi = \chi_0 + \frac{C}{T - \theta_P}, \tag{5}$$

where the temperature-independent term χ_0 may be attributed to the temperature independent van Vleck contribution which is due to the small energy difference between the ground-state multiplet $J=5/2$ and the first excited multiplet $J=7/2$. The fit yields the values for the paramagnetic Curie temperature $\theta_p=-21.3$ K and effective Sm moment $\mu_{eff}=0.87\mu_B$, which is in a good agreement with the value of $0.85\mu_B$ expected for the Sm^{3+} free ion; $\chi_0=1.15\times10^{-8}$ m^3/mol. The considerable deviation from the fit line

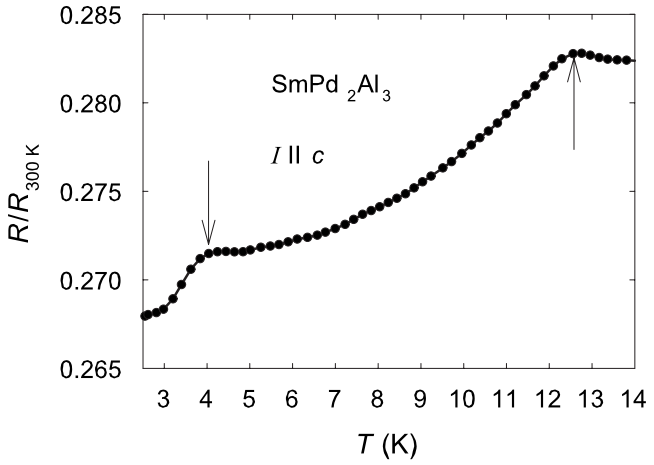

FIG. 9. Temperature dependence of relative electrical resistivity of $SmPd_2Al_3$ with electric current applied along the c axis in temperature region of magnetic phase transitions.

at higher temperatures can be attributed to population of the second excited multiplet.

To see the impact of magnetism on electrical transport we measured also the temperature dependence of the electrical resistivity for current along c (see Fig. 9). We have detected a clear cusp around 12.5 K, which is in good agreement to the onset of ferromagnetism at T_C determined by other experiments discussed above and also with results presented in the literature.[4,10] Another cusplike anomaly is seen around 4 K which coincides with T_2.

C. First-principles and CF calculations

The calculated GGA electronic DOS of $SmPd_2Al_3$, using the experimentally determined lattice parameters, is shown in Fig. 10(a). The occupied part of the DOS has a width of 9.5 eV. The first region, from −9.5 to −4.8 eV, consists mainly of the free electronlike states from the interstitial region and the Sm 6s, Pd 5s, Al 3s, and Al 3p states from AS spheres [see Figs. 10(b)–10(d)]. The following band group from −4.8 eV to the Fermi level represents mainly the Pd 4d states hybridizing with the Sm 5d and Al 3p states. The unoccupied states above the Fermi level have predominantly the Sm 5d character with an admixture of the Pd 4d and Al 3p states and the large contribution from the free electronlike interstitial region [Figs. 10(b)–10(d)]. The energy position of the localized Sm $4f^5$ states is correctly below the Fermi level. We performed also the spin-polarized LSDA and GGA calculations in order to estimate the value of the hybridization induced Pd and Al magnetic moments (4f in core and 4f in band as a Bloch states) and found values less than $0.1\mu_B$ and $0.01\mu_B$, respectively. The Fermi level for $SmPd_2Al_3$ situated at the descending part of the DOS yielded $N(E_F)=2.51$ states 1/eV (f.u.). The orbital analysis of the DOS shows that mainly the Pd 4d, Pr 5d, and Al 3p states that contribute to the total DOS at E_F. The value of the DOS at E_F is too small to cause a spontaneous magnetic polarization of the Pd 4d states. The value of the DOS at E_F for $SmPd_2Al_3$ corresponds to an electronic specific-heat coefficient $\gamma=5.9$ mJ mol^{-1} K^{-2}, which is somewhat lower than the γ value of 7.0 mJ mol^{-1} K^{-2} derived from our specific-heat data. This points to a rather low value of the mass-enhancement coefficient $\lambda=0.18$ for $SmPd_2Al_3$ [$\gamma_{exp}=(1+\lambda)\gamma_{band}$], indicating a weak electron-phonon interaction in the $SmPd_2Al_3$ compound. Next, the magnetic susceptibility was calculated on the basis of the CF scheme. The microscopic CF Hamiltonian for the Sm atomic configuration $4f^5$ in the hexagonal symmetry has four independent parameters A_n^m. Reliable CF parameters were obtained for the $NdPd_2Al_3$ compound by fitting inelastic neutron data in Refs. 13 and 14; the values obtained were $A_2^0=-386$ K, $A_4^0=42$ K, $A_6^0=6.8$ K, and $A_6^6=-134$ K. At first we decided to check these values by our first-principles calculations.

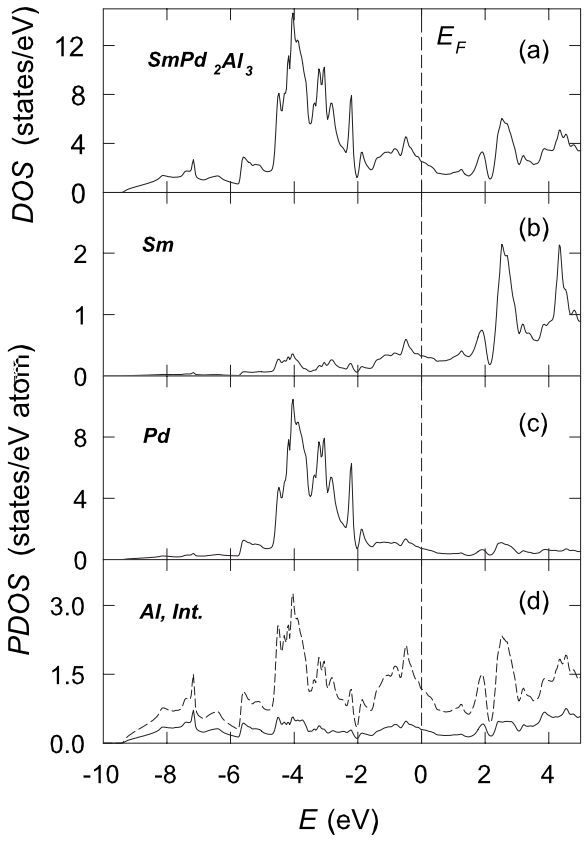

FIG. 10. Total DOS (a) and atom-projected DOS [(b)–(d)] of $SmPd_2Al_3$. The projected Sm DOS [(b) thick line], Pd [(c) thick line], Al [(d) thick line], and the interstitial region [(d) dashed line] are shown. Fermi level is put at zero energy.

The first-principles calculation of the crystal-field parameters leads to the following values: $A_2^0=-307$ K, $A_4^0=25$ K, $A_6^0=1.9$ K, and $A_6^6=-88$ K for $SmPd_2Al_3$ using the GGA form[18] of the exchange-correlation potential. When we consider spin-orbit interaction the values were: $A_2^0=-308$, $A_4^0=25$, $A_6^0=1.9$, and $A_6^6=-88$. The second-order CF parameter has the correct sign, which determines the easy c axis of $SmPd_2Al_3$ at low temperatures in agreement with the analysis of our susceptibility and magnetization data. The other parameters have also the correct sign and similar values compared to the CF parameters resulting from the analysis of inelastic neutron data in Refs. 13 and 14. Moreover the cal-

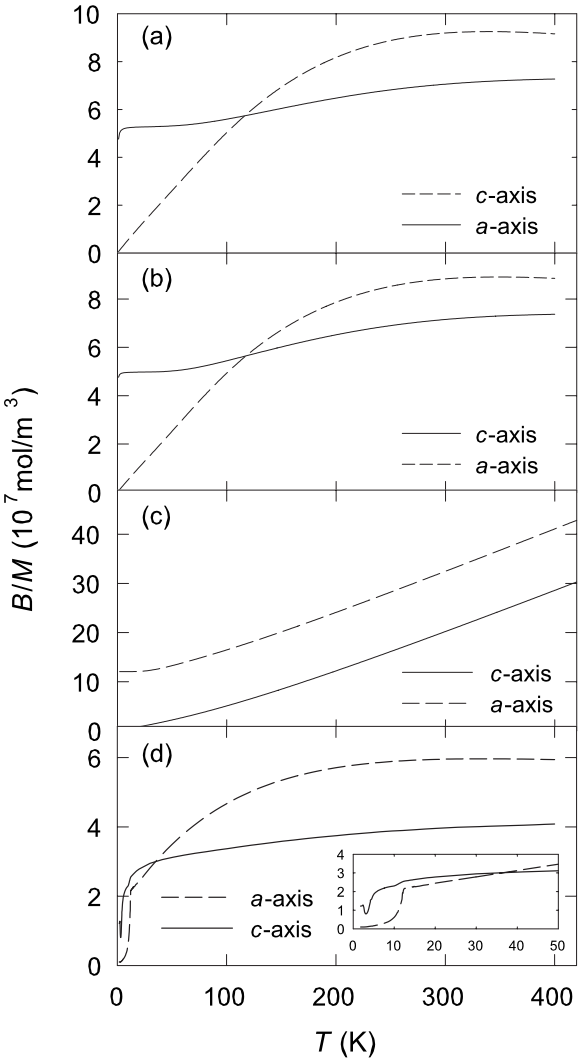

FIG. 11. Paramagnetic susceptibility as a function of temperature of $SmPd_2Al_3$ calculated using CF model (see text). Calculated curves for the CF parameters from $NdPd_2Al_3$ (a) and for our first-principles calculated CF parameters for $SmPd_2Al_3$ (b) and calculation the CF acting on the ground-state multiplet $J=5/2$ only (c). Experimental data are displayed in the bottom panel (d).

culated gap between the ground and the first excited doublet is more than 100 K, which is in good agreement with the Schottky specific-heat analysis and this fact is also supported by the reliability of both the CF parameter sets obtained above. Since our theoretical approach is semiquantitative only,[20] we may state that a consistent description of the CF interaction in $SmPd_2Al_3$ compound is obtained. We would like to emphasize that we calculated a similar temperature dependence of magnetic susceptibility, which has an intersection of curves along the *c* and *a* axes (see Fig. 11), as we found by experiment. The intersection was not obtained using the CF acting on the ground-state multiplet $J=5/2$ only so it requires at least the CF acting on $J=5/2$, $J=7/2$, and $J=9/2$ quantum subspace. Note that no intersection has been obtained from the theory published by Liu.[3]

A detailed comparison would require a correct description of the exchange interaction in the paramagnetic region above 12.6 K, since the simple molecular-field and CF model was found to provide only a semiquantitative agreement with our experimental data, and is therefore definitely too crude for a description of our measured paramagnetic susceptibility versus temperature data. Furthermore, we therefore also decided not to fit the measured data by a too-crude molecular-field and CF model approach.

IV. CONCLUSIONS

We have prepared a single crystal of the $SmPd_2Al_3$ compound in order to study specific features of Sm magnetism. The magnetization, ac susceptibility, and specific-heat measurements of the crystal exposed to magnetic fields applied along the principal crystallographic axes revealed a strong uniaxial magnetocrystalline anisotropy (even in paramagnetic state) with a easy-magnetization direction in the *c* axis, which is in contrast to the easy-plane anisotropy reported for other compounds in the $REPd_2Al_3$ group. The four magnetic transitions observed with temperature dependence of the specific heat at temperatures $T_3=3.4$ K, $T_2=3.9$ K, $T_1=4.4$ K, and $T_C=12.4$ K, respectively, and detected in part also in magnetization, ac susceptibility, and electrical resistivity data, point to a complex magnetic phase diagram for $SmPd_2Al_3$. Although this material becomes ferromagnetic below $T_C=12.4$ K, an antiferromagnetic ground state seems to become established at low temperatures. The series of four metamagnetic transitions detected at 0.03, 0.35, 0.5, and 0.75 T, respectively, underlines the complexity of the Sm magnetism, which is characterized by a small Sm magnetic moment and a complex interplay of crystal-field and exchange interactions. The principal role of CF interaction has been confirmed by *ab initio* calculations and our comparison of calculated and experimental paramagnetic susceptibility data. To prove the validity of our scenario on the multiphase magnetic diagram, as well as on the magnetic phase transitions indicated in our work suitable microscopic experiments are strongly desired; namely, neutron diffraction and μSR spectroscopy. The high neutron absorption by Sm for a standard thermal neutron wavelength implies that a hot neutron beam would be necessary for a successful neutron-diffraction experiment with the $SmPd_2Al_3$ crystal.

ACKNOWLEDGMENTS

This work is part of research plan MSM 0021620834 financed by the Ministry of Education of the Czech Republic. This work was also supported by grants of the Czech Science Foundation under Grants No. 202/09/1027 and No. 202/09/P354, and the Grant Agency of Charles University under Grant No. 150407.

*jiri.pospisil@centrum.cz

[1] G. H. Dieke, *Spectra and Energy Levels of Rare Earth Ions in Crystals* (John Wiley & Sons, USA, 1968).
[2] H. de Wijn, A. van Diepen, and K. Buschow, Phys. Rev. **161**, 253 (1967).
[3] Z. Liu, Phys. Rev. B **64**, 144407 (2001).
[4] H. Kitazawa, A. Mori, S. Takano, T. Yamadaya, A. Matsushita, and T. Matsumoto, Physica B **186-188**, 661 (1993).
[5] C. Geibel, C. Schank, S. Thies, H. Kitazawa, C. Bredl, A. Bohm, M. Rau, A. Grauel, R. Caspary, R. Helfrich, U. Ahlheim, G. Weber, and F. Steglich, Z Phys. B: Condens. Matter **84**, 1 (1991).
[6] V. S. Zapf, R. P. Dickey, E. J. Freeman, C. Sirvent, and M. B. Maple, Phys. Rev. B **65**, 024437 (2001).
[7] S. Mentink, N. Bos, G. Nieuwenhuys, A. Menovsky, and J. Mydosh, Physica B **186-188**, 497 (1993).
[8] H. Ghosh, S. Ramakrishhnan, A. Chinchure, V. Marathe, and G. Chandra, Physica B **223-224**, 354 (1996).
[9] S. Suga, M. Takeda, Y. Mori, N. Shino, S. Imada, and H. Kitazawa, Physica B **186-188**, 63 (1993).
[10] K. Ghosh, S. Ramakrishnan, S. K. Malik, and G. Chandra, Phys. Rev. B **48**, 6249 (1993).
[11] A. Donni, H. Kitazawa, P. Fischer, T. Vogt, A. Matsushita, Y. Iimura, and M. Zolliker, J. Solid State Chem. **127**, 169 (1996).
[12] G. Motoyama, T. Nishioka, and N. Sato, J. Phys. Soc. Jpn. **71**, 1609 (2002).
[13] A. Donni, A. Furrer, H. Kitazawa, and M. Zolliker, J. Phys.: Condens. Matter **9**, 5921 (1997).
[14] A. Dönni, A. Furrer, E. Bauer, H. Kitazawa, and M. Zolliker, Z. Phys. B: Condens. Matter **104**, 403 (1997).
[15] H. Rietveld, J. Appl. Crystallogr. **2**, 65 (1969).
[16] http://www.ill.eu/sites/fullprof/
[17] J. P. Perdew and Y. Wang, Phys. Rev. B **45**, 13244 (1992).
[18] J. P. Perdew, K. Burke, and M. Ernzerhof, Phys. Rev. Lett. **77**, 3865 (1996).
[19] P. Blaha, K. Schwarz, G. Madsen, D. Kvasnicka, and J. Luitz, www.wien2k.at, 2001.
[20] M. Diviš, J. Rusz, H. Michor, G. Hilscher, P. Blaha, and K. Schwarz, J. Alloys Compd. **29**, 403 (2005).
[21] V. Nekvasil, M. Diviš, G. Hilscher, and E. Holland-Moritz, J. Alloys Compd. **225**, 578 (1995).
[22] P. Svoboda, P. Javorský, M. Diviš, V. Sechovský, F. Honda, G. Oomi, and A. A. Menovsky, Phys. Rev. B **63**, 212408 (2001).
[23] J. Vejpravová, P. Svoboda, M. Rotter, M. Doerr, and M. Loewenhaupt, Physica B **329-333**, 504 (2003).
[24] M. Schwerin, B. Becker, A. Eichler, and J. A. Mydosh, J. Magn. Magn. Mater. **226-230**, 176 (2001).
[25] P. Svoboda, J. Vejpravová, S. Daniš, and M. Mihalik, Physica B **378-380**, 1107 (2006).
[26] M. Fisher, Philos. Mag. **7**, 1731 (1962).
[27] M. El-Hagary, M. Michor, and G. Hilscher, Physica B **284-288**, 1489 (2000).